International Journal for Multidisciplinary Research (IJFMR)
E-ISSN: 2582-2160 ● Website: www.ijfmr.com ● Email: editor@ijfmr.com

Fractional-Order Inverse Filter Design by Using Second Generation Voltage Conveyor

Pothumudi Hema Vinay Kumar[1], Tirumala Krishna Battula[2]

[1]VLSI &ES, University College of Engineering Kakinada, Kakinada, India
[2]Department of ECE, University College of Engineering Kakinada, India

ABSTRACT
In this study, we introduce low-pass and high-pass inverse filter configurations that provide both simplicity and the capability to independently adjust gain and characteristic frequency. The second-generation voltage conveyor (VCII) offers these benefits because of its distinctive terminal features. Additionally, we explore potential applications for these types of RC filters. We use Cadence's IC design suite to do a frequency analysis on a control system that incorporates these filters in order to evaluate its performance.

KEYWORDS: Fractional order filters, second generation voltage conveyor, inverse filter, resistance, capacitor.

1. INTRODUCTION

Inverse filters, which are the inverse of traditional filters like low pass, high pass, and band pass, have a frequency response that is the inverse of the original [1]. Although there is a plenty of literature on second-order inverse filter architectures, first-order structures are not as well-documented. Particularly, recent advancements have led to the development of current-mode inverse all-pass filters employing four-terminal floating nullor (FTFN) and current differencing transconductance amplifiers (CDTAs) [3,4]. These developments have prompted research into the realization of low-pass and high-pass filter configurations, utilizing operational amplifiers (op-amps) as the active components. This exploration is conducted within the framework of voltage-mode inverse all-pass filters that rely on second-generation current conveyors (CCIIs) [5].

The originality of this study resides in the development of voltage-mode backwards low-pass and high-pass channel designs that utilization a solitary VCII as the dynamic component. When compared to earlier topologies, this drastically lowers the necessary number of active components. While the equivalent topologies suggested previously need just a single op-amp, the proposed designs provide more design freedom by enabling separate modifications of the key frequency properties [6].

Additionally, we conduct a systematic comparison with relevant existing structures. We explore potential applications of these filter types to demonstrate their practical value. Utilizing the Rhythm IC plan suite and the plan pack provided by Austria Mikro Systeme (AMS) for the 0.45 m CMOS process, we choose a control system to serve as an example design and evaluate its performance via simulation results.

2. FRACTIONAL-ORDER INVERSE FILTERS

A partial request low-pass channel or high-pass channel are examples of transfer functions that may be expressed as fractional-order differential equations.

Precisely, the transfer function of the fractional-order ILP filter is as follows:

$$H_{ILP}(s) = K \cdot [1 + (\tau s)]. \quad (1)$$

With τ acting as a time constant and $0 < \mu < 1$ representing the filter's order.

Using the setting $s^{\mu} = \omega^{\mu} \cdot [\cos(0.5\pi\mu) + \sin(0.5\pi\mu)]$, the phase and magnitude responses' derived formulas are

$$|H_{ILP}(\omega)| = K \cdot \sqrt{1 + (\omega\tau)^{2\mu} + 2(\omega\tau)^{\mu} \cos(0.5\pi\mu)}. \quad (2)$$

$$\angle H_{ILP}(\omega) = \tan^{-1}\left[\frac{(\omega\tau)^{2\mu}\sin(0.5\pi\mu)}{1+(\omega\tau)^{\mu}\cos(0.5\pi\mu)}\right]. \quad (3)$$

The increase of the channel is equivalent to K at its lowest frequencies. However, at the high frequencies, it exhibits the behaviour of a partial request differentiator, with a steady stage of $0.5\pi\mu$ and a frequency response slope of $+6\mu$dB/Oct.

Consider of a IHP filter with fractional order

$$H_{ILP}(s) = K \cdot \frac{(\tau s)^{\lambda}+1}{(\tau s)^{\lambda}} \quad (4)$$

where the order is $0 < \lambda < 1$. In the same way as with the ILP channel, the addition and stage recurrence reactions may be expressed as expressions,

$$|H_{IHP}(\omega)| = K \cdot \frac{\sqrt{1+(\omega\tau)^{2\lambda}+2(\omega\tau)^{\lambda}\cos(0.5\pi\lambda).}}{(\omega\tau)^{\lambda}}. \quad (5)$$

$$\angle H_{IHP}(\omega) = -0.5\pi\lambda + \tan^{-1}\left[\frac{(\omega\tau)^{\lambda}\sin(0.5\pi\lambda)}{1+(\omega\tau)^{\lambda}\cos(0.5\pi\lambda)}\right]. \quad (6)$$

At low frequencies, the filter functions as a partial request integrator, with a stage of $-0.5\pi\lambda$ and a slope of -6λdB/Oct. The gain tends to K in the high frequency range.

3. FILTER DESIGN USING SECOND GENERATION VOLTAGE CONVEYOR

As can be seen in Figure.1, the Voltage Transport is a three-port simple structure block with the Y, X, and Z ports linked as shown.

$$Vz = \alpha Vx$$
$$Ix = -\beta Iy$$

The VCII consists of a current follower that routes current from the low-impedance, virtually grounded terminal Y to terminal X, and a voltage supporter that courses voltage from terminal X to the low-yield impedance, basically grounded terminal Z. The input and output terminals of these CCII dual circuits have a low impedance. Most notably, unlike CCIIs, which need an additional buffer to be placed at their outputs [7–13], VCII-based stages may be connected in a cascade. A VCII is represented by its related symbol in Figure.1, whereas the full scale model of a non-ideal VCII, with parasitic impedances added to every terminal, is shown in Figure.2. Behaviour of a VCII may be described using the matrix equation below.

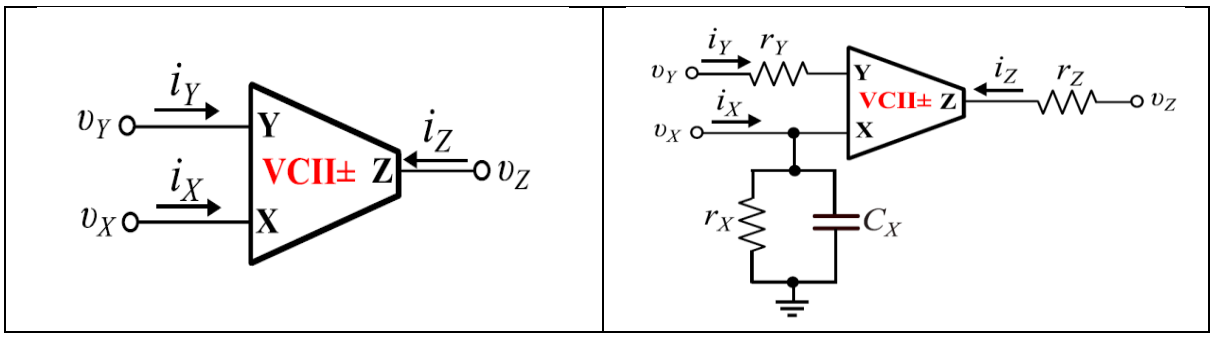

Figure 1. Symbol for a second-generation voltage conveyor	Figure 2: The VCII macro-model with the corresponding parasitic impedance

For a VCII, the current carrying action between terminals Y and X is characterised by the variable β, while the voltage conveying activity between terminals X and Z is described by the factor.

$$\begin{bmatrix} i_X \\ v_Z \\ v_Y \end{bmatrix} = \begin{bmatrix} -\alpha & \frac{1}{r_x // \frac{1}{C_X s}} & 0 \\ 0 & \beta & r_z \\ r_y & 0 & 0 \end{bmatrix} . \begin{bmatrix} i_Y \\ v_X \\ i_Z \end{bmatrix}$$

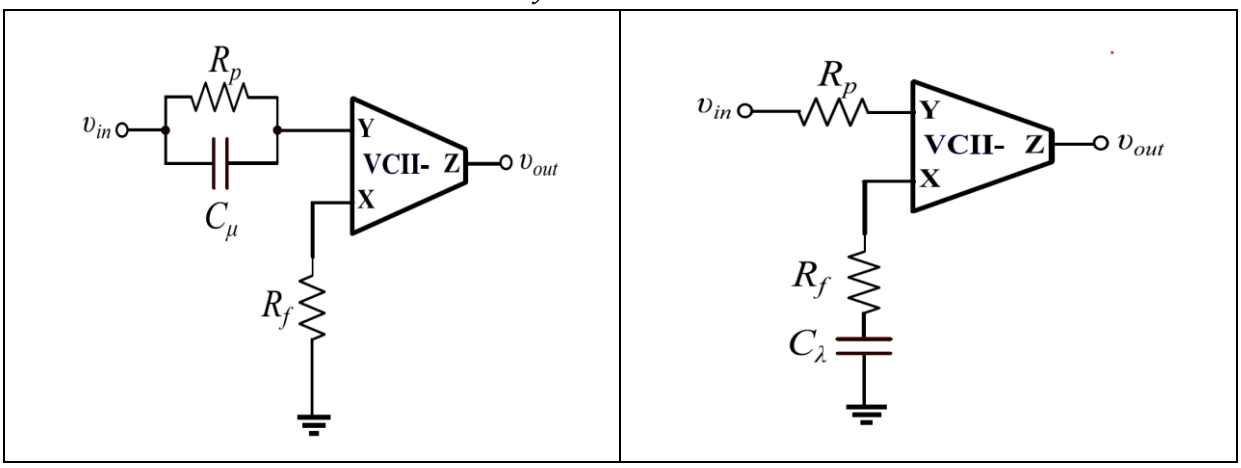

Fig. 3. VCII inverse filter implementation, with (A) low pass and (B) high pass

Figure. 3A shows how the transfer function in (1) is implemented. The voltage carrier of the second generation with a negative sign (VCII-) is the active element used in this example. utilizing a pseudo-capacitance's impedance expression. The transfer function that is being used is provided by(7).

$$H_{ILP}(s) = \frac{R_f}{R_p} . \left(1 + R_p C_\mu s^\mu\right). \quad (7)$$

Where as

$$\mathrm{K} = \frac{R_f}{R_p}, \tau = (R_p C_\mu)^{\frac{1}{\mu}}. \quad (8)$$

A fractional-order IHP filter is shown in motion in Figure 3B, and its realised transfer function is

$$H_{IHP}(s) = \frac{R_f}{R_p} . \frac{R_f C_\lambda s^\lambda + 1}{R_f C_\lambda s^\lambda}. \quad (9)$$

Where as

$$\mathrm{K} = \frac{R_f}{R_p}, \tau = \left(R_f C_\lambda\right)^{\frac{1}{\lambda}}. \quad (10)$$

The exchange capability of the channel establishes the connection between the input and output signals. For the topology you have selected, use standard filter design formulas and methodologies. The VCII settings and passive component (capacitors, resistors) values to satisfy the filter design specifications. This includes figuring out the values of the capacitor and resistor to set the time constants of the filter. VCII settings to maximize the efficiency of the filter. Modify the component values according to the measures.

4. IMPLEMENTATION OF FRACTIONAL ORDER INVERSE FILTER USING VCII

Figure 3(A) is the circuit that will be used to realise the transfer function in (7,9), by utilizing the design equations in (8,10). The resistor values are Rf = 40 kΩ and Rp = 20 kΩ, and the integer-order

capacitor value for $C\mu*$ = 100 µF. Figure 4 shows the design of the VCII architecture that will be used in the simulations. Table 1 provides MOS transistor aspect ratios based on MOS transistors produced using the AMS 0.45 µ m CMOS innovation. It was resolved that the dc predisposition current (I_0) was 20 An and that the dc power supply voltages were VDD = - VSS = 1.5 V.

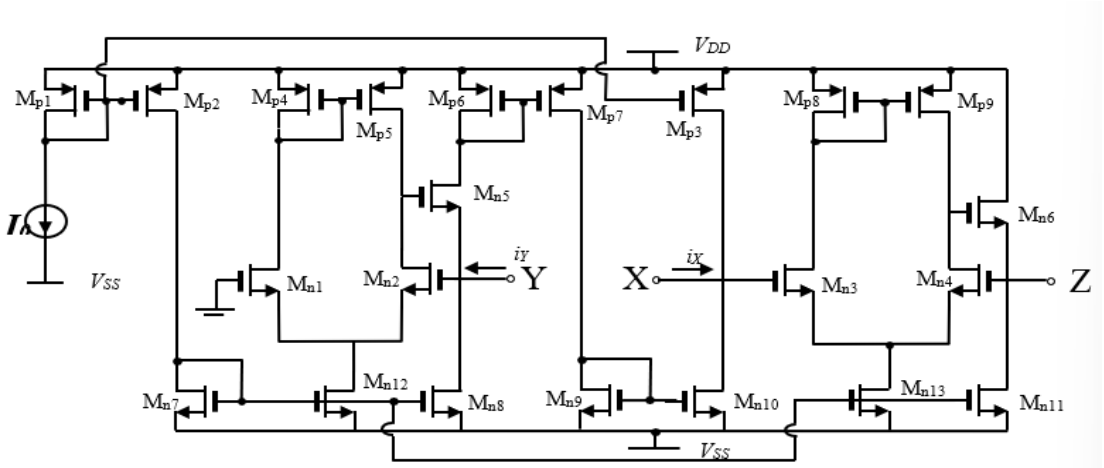

Figure. 4. Schematic circuit of second generation voltage conveyor (VCII-)

Transistor	Aspect ratio
Mp1- Mp9	30 µm/2 µm
Mn1- Mn4	20 µm/2 µm
Mn5- Mn6	20 µm/0.4 µm
Mn7- Mn11	2 µm/2 µm
Mn12- Mn613	4 µm/2 µm

Table 1: VCII Aspect Ratios of MOS Transistors –

Furthermore, we conducted measurements to assess the impact of process, power supply voltage, and temperature (PVT) corners on the phase margin and setup time of the control system. In pursuit of this objective, we took into account the MOS transistor corners characterized by both speed (fast nMOS - slow pMOS, worst case 1) and slow (slow nMOS - fast pMOS, worst case 0), as well as power (fast nMOS - fast pMOS, worst case wp) and slow (slow nMOS - slow pMOS). The temperature corners were set at 0 and 60 degrees Celsius, and the power supply voltage corners were set at (VDDVSS) 10%.

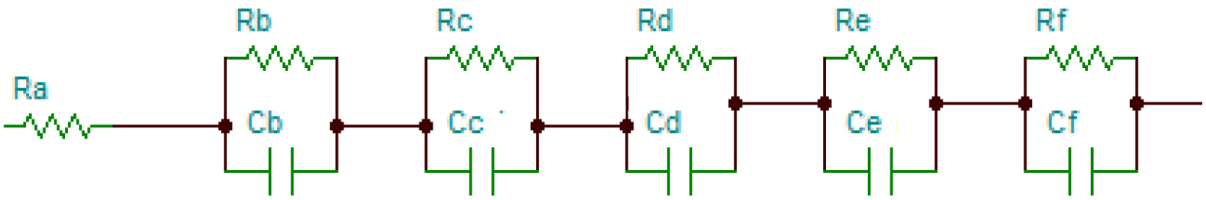

Figure. 5. passive realization of fifth order approximation

$$H(s) = R_a + \frac{1}{sC_b+R_b} + \frac{1}{sC_c+R_c} + \cdots \quad (11)$$

In order to passively realize a fifth-order system, you would have to design a circuit that uses passive parts and displays the desired characteristic equation or transfer function. This transfer function, which is

commonly expressed as H(s) in the Laplace domain with "s" standing for the complex frequency variable, clarifies how internal signals are related to those at the system's input and output. The transfer function, in its simplest form, represents the connection between the framework's feedback and result signals.

5. APPLICATION DESIGN EXAMPLE

The fractional-order capacitor's behaviour is represented in Fig. 5 [14] by a Foster type-II network. Considering a frequency range of [10^{-1}-10^{+2}] rad/sec, Figs. 7(A) and 7(B) show the gain and phase responses of the capacitor C=100 F for various orders of approximation, respectively. It seems from the associated graphs that the fifth request Oustaloup estimation [15] is a feasible option for accomplishing adequate accuracy in both the addition and stage reactions.

S.No	Component	Numerical values
1	Ra	0.2115 Ω
2	Rb	0.2593 Ω
3	Rc	0.2541 Ω
4	Rd	0.3363 Ω
5	Re	0.6442 Ω
6	Rf	3.0219 Ω
7	Cb	0.2810 f
8	Cc	1.4662 f
9	Cd	3.5968 f
10	Ce	6.5493 f
11	Cf	11.2930 f

Table. 2. The RC network's element values are shown in fig. (), which can be used to replace the fig(3)'s fractional order capacitor

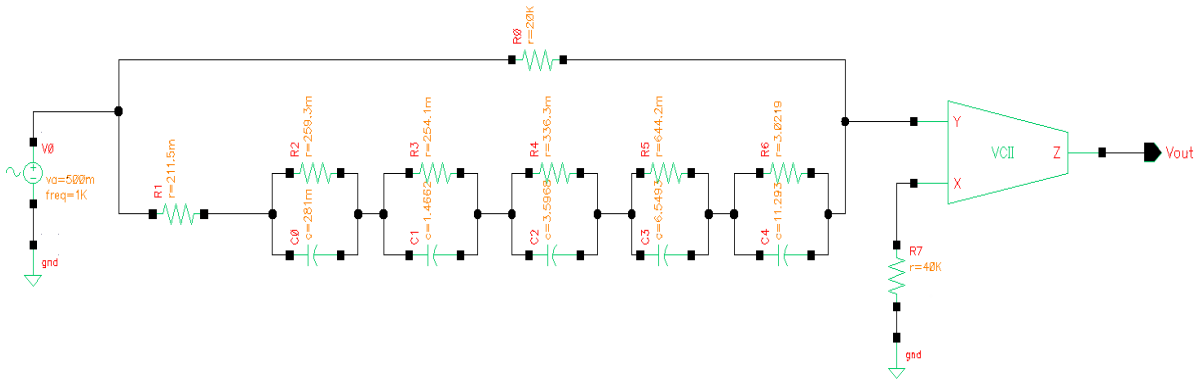

(A)

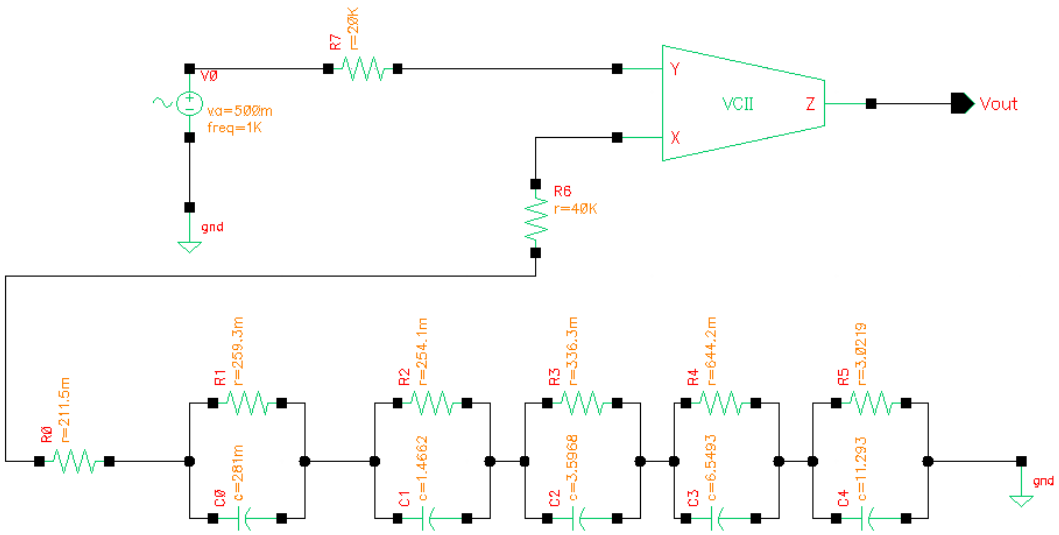

(B)

Figure. 6. Proposed Fractional order in (A) ILP filter (B) IHP filter.

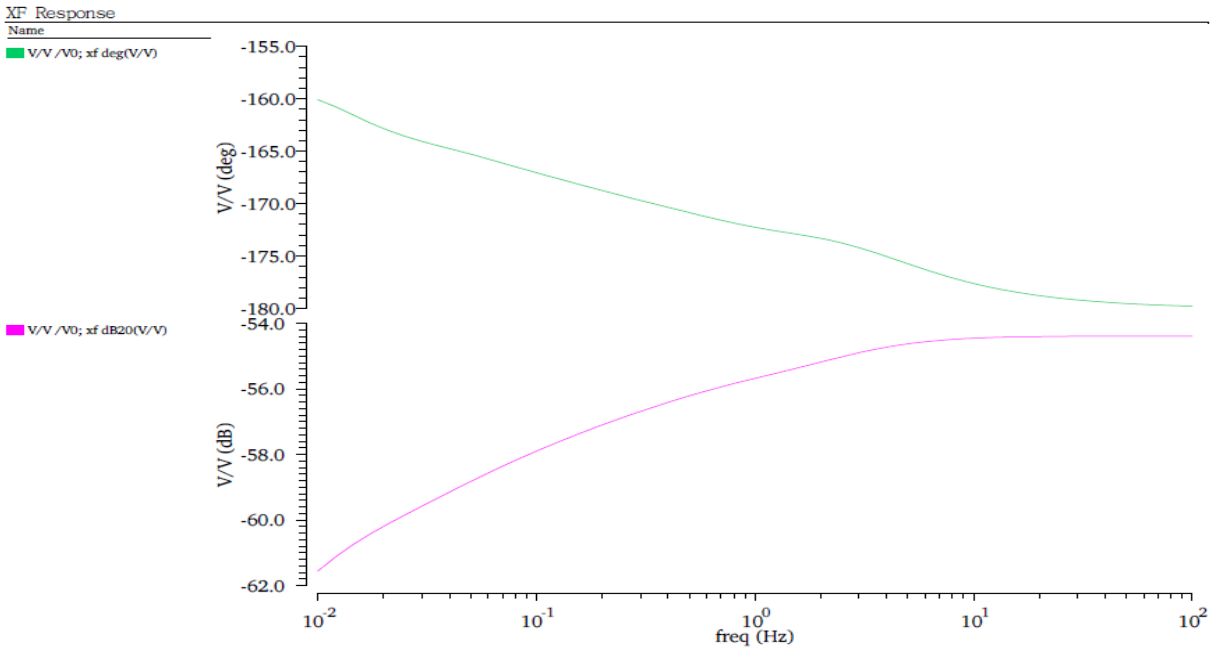

(A)

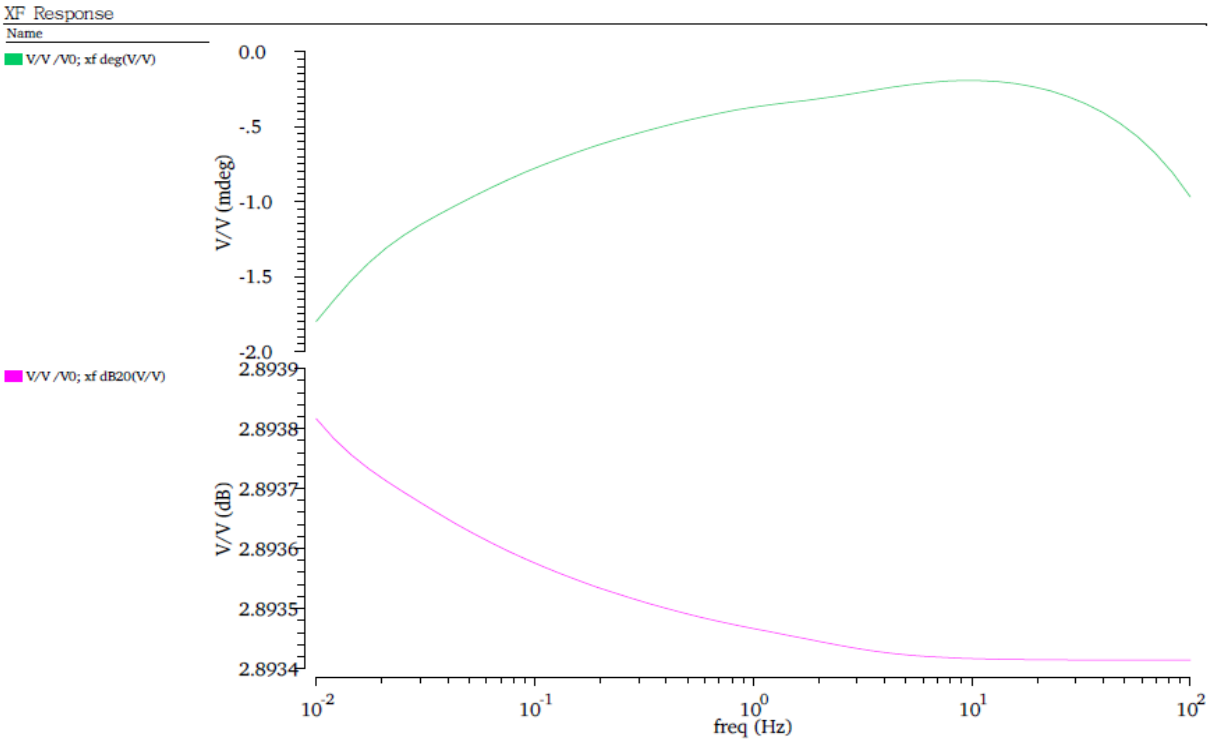

(B)

Figure. 7. Frequency response in Phase and Gain of the (A) ILP circuit (B) IHP circuit

In comparison to the theoretical values of 72˚ and 22.5rad/sec, 25dB and 4.5rad/sec, the frequency responses of the simulated values ($10^{-1} - 10^{+2}$) frequency of the gain and phase are settling time in 71.7˚ and 20.49rad/sec, 23.1dB and 3.89rad/sec.

The transient analysis tool (t = 200 nSec) provided by the Analogue Design Environment has been used to assess the system's sensitivity performance. The resulting reaction in terms of voltage and current is shown in the image. As can be seen in Figures 8A and 8B, the sensitivity characteristics offered by the given implementation are rather respectable.

The input voltage Va is 500m, 1K Hz, and the output voltage VCC-VDD. Figure 9A and 9B show two parallel graphs that correlate to each other. In light of the above, it may be concluded that the impact of PVT corners on framework execution is negligible.

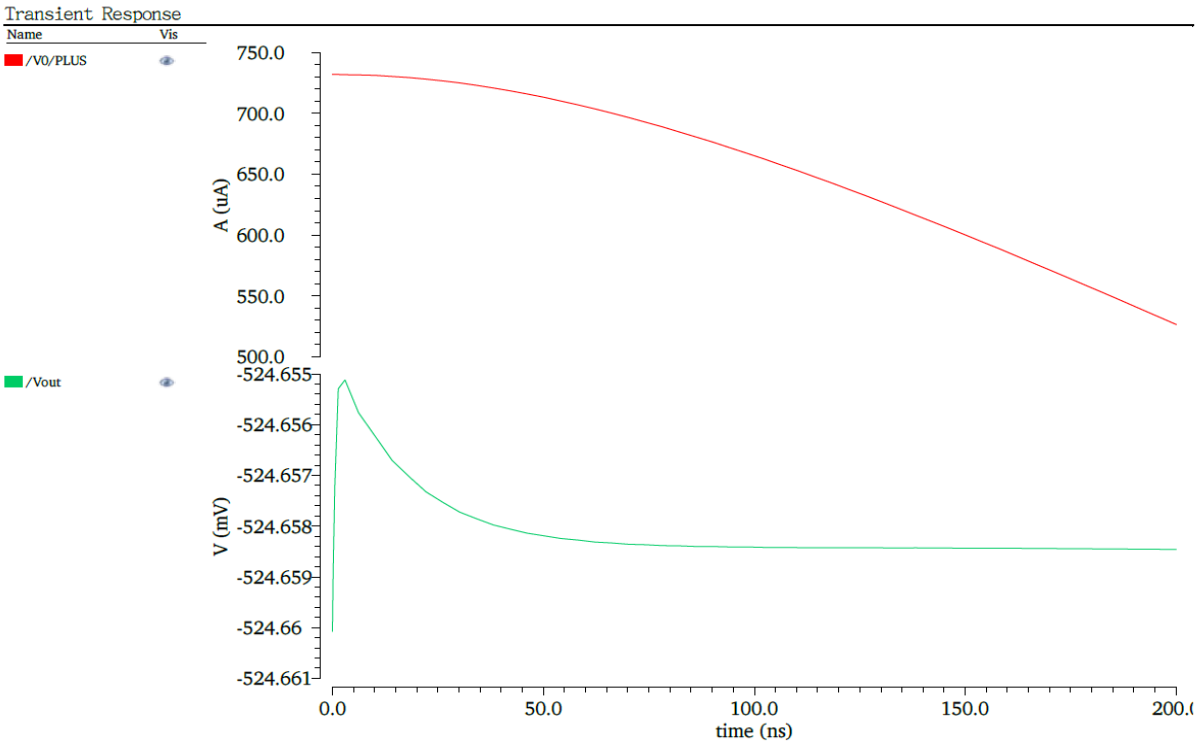

(A)

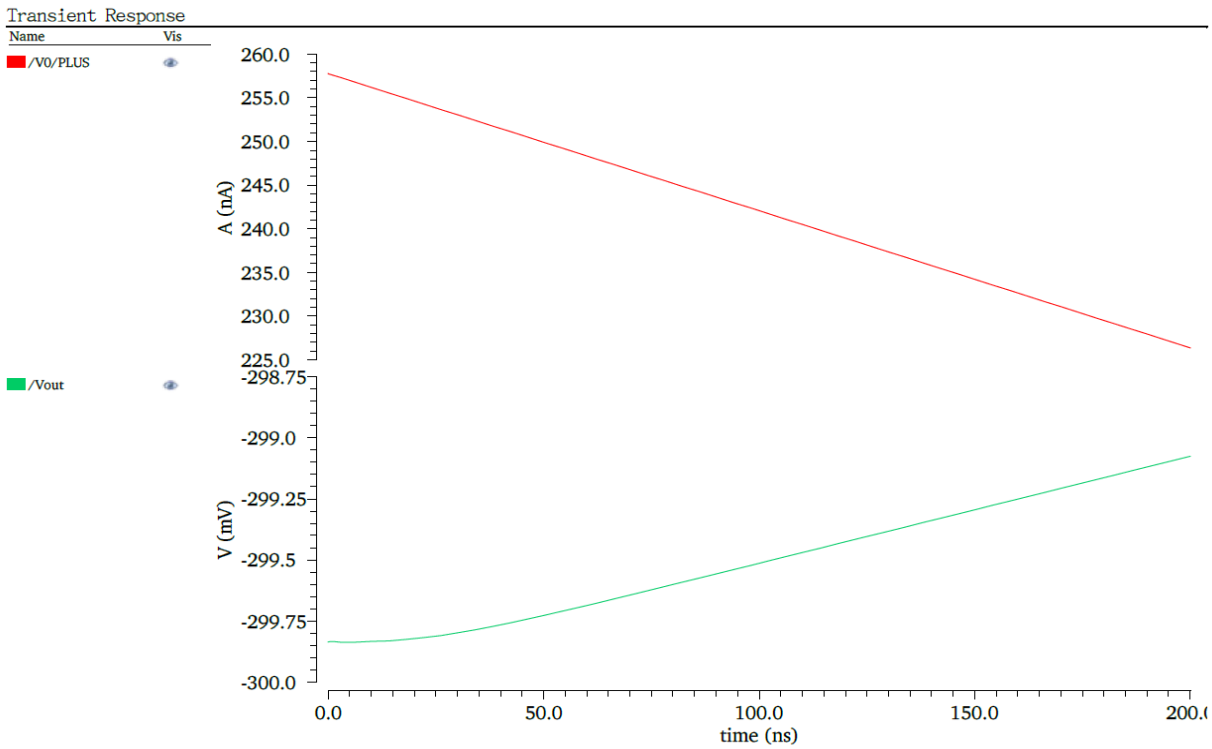

(B)

Figure. 8. Transient responses of the (A) ILP filter (B) IHP filter

6. CONCLUSION

To implement the suggested fractional-order inverse filter design, a novel circuit based on the second-generation voltage conveyor (VCII) is presented. The suggested filters were first modelled using

a VCII block, a voltage conveyor of the second generation. One of the approximations is used to find the RC values is applied to the VCII based CMOS schematic. Further, frequency analysis has been done for the proposed filters. The suggested filters have been simulated in Cadence Virtuoso, and the results have been confirmed. So Cadence results is improved into the previous frequency analysis of phase and gain response of fractional order inverse filters.

7. REFERENCES

1. Psychalinos, Costas & Minaei, Shahram & Yesil, Abdullah. (2022). First order inverse filters: Implementations using a single voltage conveyor and potential applications. International Journal of Circuit Theory and Applications. doi: 50. 10.1002/cta.3346.
2. Shah NA, Malik MA. FTFN based dual inputs current-mode allpass inverse filters. Indian J Pure Appl Sci. 2005;34:206-209. http://nopr.niscair.res.in/bitstream/123456789/25662/1/IJRSP%2034%283%2%9%20206-209.pdf
3. Shah NA, Quadri M, Iqbal SZ. High output impedance current-mode allpass inverse filter using CDTA. Indian J Pure Appl Sci. 2008;46: 893-896. http://nopr.niscair.res.in/handle/123456789/3057
4. Shah NA, Rather MF. Realization of voltage-mode CCII-based allpass filter and its inverse version. Indian J Pure Appl Sci. 2006;44:269-271. http://nopr.niscair.res.in/handle/123456789/8297
5. Kamat DV. New operational amplifier based inverse filters. In: 3rd International conference on Electronics, Communication and Aerospace Technology (ICECA); 2019:1177-1181. doi:10.1109/iceca.2019.8821898
6. Safari L, Barile G, Stornelli V, Ferri G. An overview on the second generation voltage conveyor: features, design and applications. IEEE Trans Circ Syst II: Express Briefs. 2018;66(4):547-551. doi:10.1109/tcsii.2018.2868744
7. Safari L, Barile G, Ferri G, Stornelli V. Traditional op-amp and new VCII: a comparison on analog circuits applications. AEU-Int J Electron Commun. 2019;110:152845. doi:10.1016/j.aeue.2019.152845
8. Yesil A, Minaei S. New simple transistor realizations of second-generation voltage conveyor. Int J Circ Theory Appl. 2020;48(11):2023-2038. doi:10.1002/cta.2879
9. Barile G, Safari L, Pantoli L, Stornelli V, Ferri G. Electronically tunable first order AP/LP and LP/HP filter topologies using electronically controllable second generation voltage conveyor (CVCII). Electronics. 2021;10(7):822. doi: 10.3390/electronics10070822
10. Stornelli V, Safari L, Barile G, Ferri G. A new VCII based grounded positive/negative capacitance multiplier. AEU-Int J Electron Commun. 2021;137:153793. doi: 10.1016/j.aeue.2021.153793
11. Yesil A, Minaei S, Psychalinos C. 0.45V CMOS second-generation voltage conveyor based on super source follower. Circ Syst Signal Proc. 2022;41:1819-1833. doi:10.1007/s00034-021-01867-7
12. Yuce E, Safari L, Minaei S, Ferri G, Barile G, Stornelli V. A new simulated inductor with reduced series resistor using a single VCII .Electronics. 2021;10(14):1693. doi:10.3390/electronics10141693
13. G. Tsirimokou, C. Psychalinos, A. Elwakil, Design of CMOS Analog Integrated Fractional-Order Circuits: Applications in Medicine and Biology, Springer, 2017, http://dx.doi.org/10.1007/978-3-319-55633-8.
14. B.T. Krishna. Realization of Fractance Device using Fifth Order Approximation. Communications on Applied Electronics. 7, 34 (Sep 2020), 1-5. DOI:10.5120/cae2020652869
15. L. Safari, E. Yuce, S. Minaei, G. Ferri, V. Stornelli, A second-generation voltage conveyor (VCII)–

based simulated grounded inductor, Int. J. Circuit Theory Appl. 48 (7) (2020) 1180–1193, http://dx.doi.org/10.1002/cta.2770.

16. R. Senani, D.R. Bhaskar, A. Raj, Inverse analog filters: History, progress and unresolved issues, Electronics 11 (6) (2022) 841, http://dx.doi.org/10.3390/electronics11060841.
17. D. Bhaskar, M. Kumar, P. Kumar, Fractional order inverse filters using operational amplifier, Analog Integr. Circuits Signal Process. 97 (1) (2018) 149–158, http://dx.doi.org/10.1007/s10470-018-1287-1.
18. D. Bhaskar, M. Kumar, P. Kumar, Minimal realization of fractional-order inverse filters, IETE J. Res. (2020) 1–14, http://dx.doi.org/10.1080/03772063.2020. 1803770.